Advanced Dynamically Adaptive Algorithms for Stochastic Simulations on Extreme Scales

Presented by

Rick Archibald, Ralf Deiterding, and Cory Hauck

Oak Ridge National Laboratory

Dongbin Xiu

Purdue University

Outline

- Capturing high dimensional complex stochastic systems
  - Generalized polynomial chaos (gPC)
  - AMR on Cartesian lattices
  - Leading adaptation with detection methods in high dimension
- Uncertainty applications
  - Reference application
  - Climate application
  - Fusion application

Capturing high dimensional complex stochastic systems

Necessary components:

- **Extension of deterministic adaptive mesh refinement (AMR) algorithms to high dimensional random space to facilitate adaptive stochastic simulations**
- **Extension of edge-detection methods to stochastic spaces to identify and locate smooth sub-domains**
- **Develop advanced, dynamically adaptive, stochastic collocation methods in smooth sub-domains. These methods will be suitable for extreme-scale computing where only finite computing resources are available**

gPC formulation and solution

The goal of capturing the uncertainty and dynamics of a physical system can be approached mathematically by determining the stochastic quantity

$$u(x,t,Z) : \bar{D} \times [0,T] \times \mathbb{R}^{n_z} \rightarrow \mathbb{R}, \tag{1}$$

which is the solution of the stochastic partial differential equation

$$\begin{cases} u_t(x,t,Z) = \mathcal{L}(u), & D \times (0,T] \times \mathbb{R}^{n_z}, \\ \mathcal{B}(u) = 0, & \partial D \times [0,T] \times \mathbb{R}^{n_z}, \\ u = u_0, & D \times \{t=0\} \times \mathbb{R}^{n_z}, \end{cases} \tag{2}$$

where $\mathcal{L}$ is a (nonlinear) differential operator, $\mathcal{B}$ is the boundary condition operator, u_0 is the initial condition, and $Z = (Z_1, \ldots, Z_{n_z}) \in \mathbb{R}^{n_z}, n_z \geq 1$, are a set of independent random variables with probability density function (PDF) ρ(z) characterizing the random inputs to the governing equation

AMR on Cartesian lattices

Mesh and corresponding local quad-tree of a structured mesh refinement strategy (*d* = 2, r = 2)

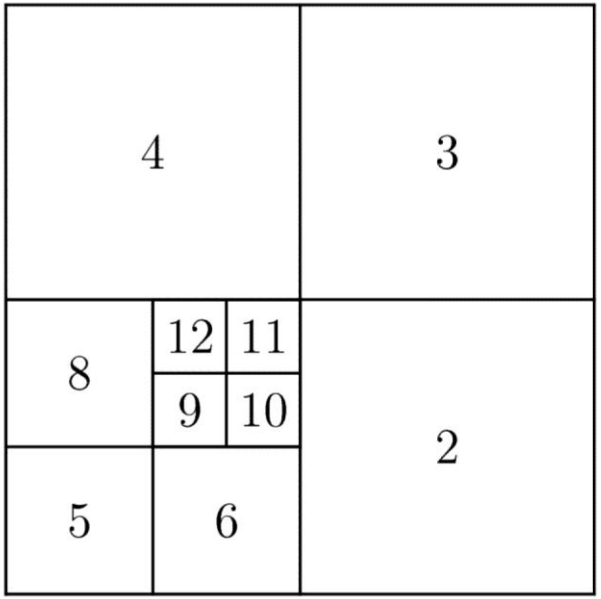

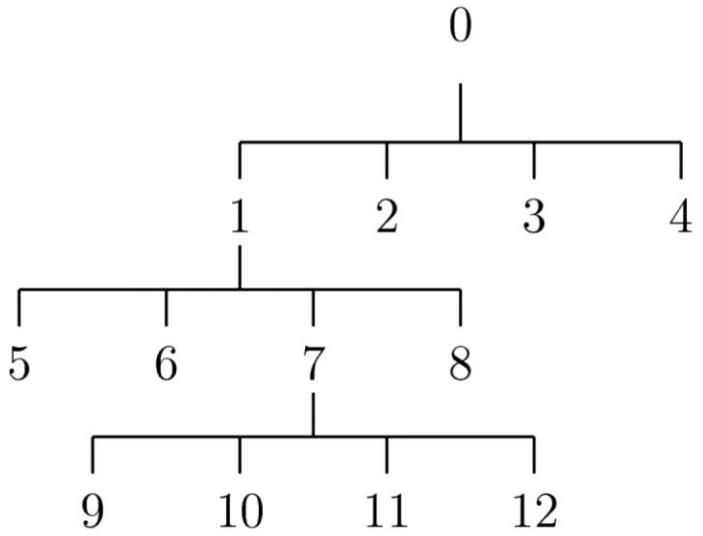

Sparse grids on Cartesian lattices

We are aiming at combining sparse grid data structures on Cartesian lattices with patch-based data representation utilizing and extending our block-structured AMR system AMROC

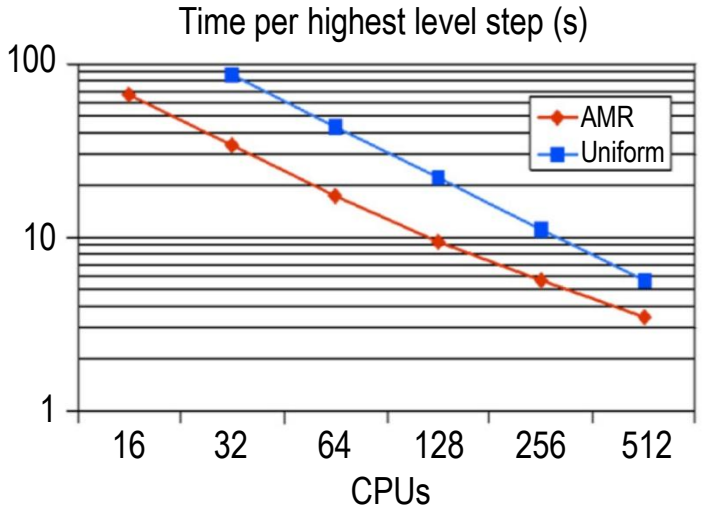

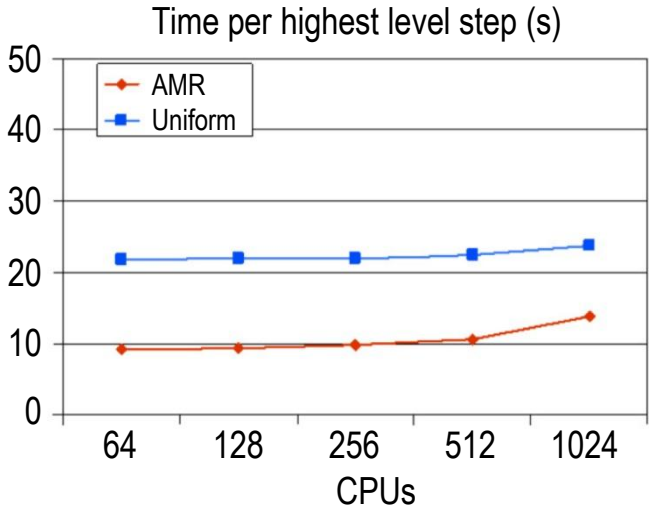

Here we present strong (left) and weak (right) scaling data of AMROC for a typical 3D spherical shock wave explosion benchmark hierarchically refined adaptively

Leading adaptation with detection methods in high dimension

We have developed functionals, for a given order *m*, that act on functions, *G*(*z*), such that

$$L_m G(z) = \begin{cases} [G](\xi) + \mathcal{O}(h(z)), & \text{if } z_{j-1} \leq \xi, z \leq z_j, \\ \mathcal{O}(h^m(z)), & \text{if } G \in \mathcal{C}^m(I_z), m > 0. \end{cases} \quad (3)$$

These functionals determine the level of smoothness of the underlying function given an arbitrary sampling of points. Thus we can generate a locally adaptive approach and refine only in non-smooth regions, thereby spending more effort in regions that likely contain discontinuities and/or shocks

Leading adaptation with detection methods in high dimension (continued)

Consider the simple function

$$G(\mathbf{z}) = \begin{cases} 1, & \sum_{i=1}^{k} z_i^2 < r^2, \ k \leq d \\ 0, & \text{otherwise.} \end{cases} \qquad (4)$$

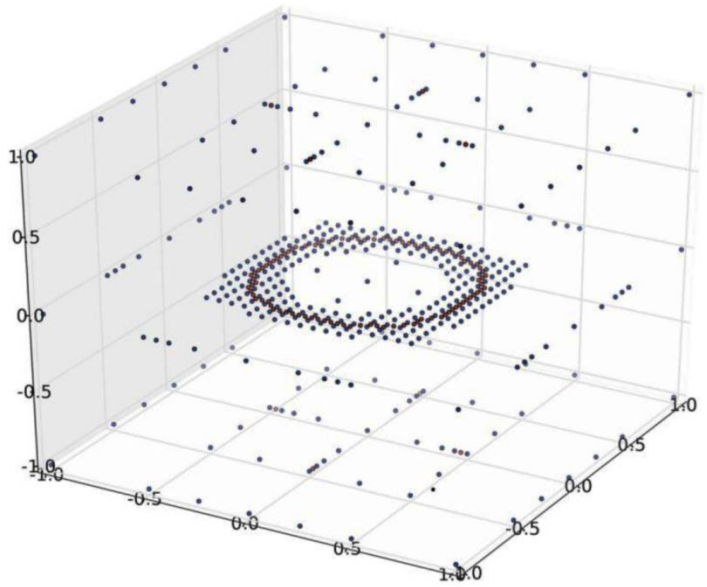

Resolved adaptive sparse grid for the function given in (4) with $d = 3$, $k = 2$, $r = 1/8$ and $\delta = 2^{-4}$

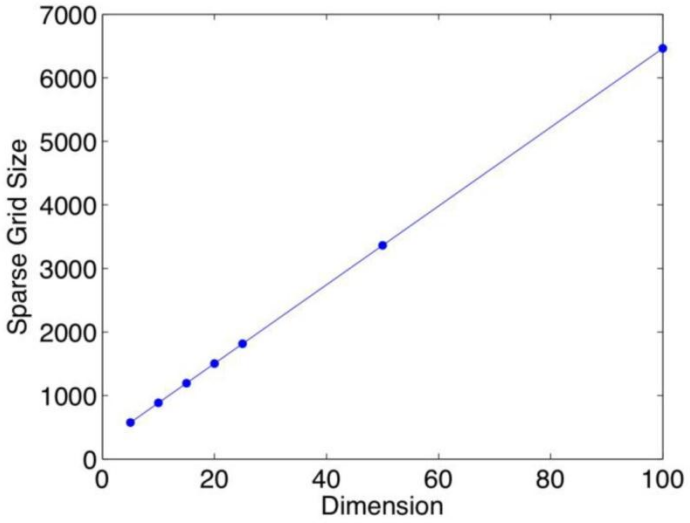

The number of points required to resolve this function as dimensionality increases

Pro-typical analytic problems

Testing against analytic problems will ensure that the proposed methods capture the complex dynamics that can exist in stochastic spaces and demonstrate the scalability and performance of the software tools

$$G(\mathbf{z}) = G_{\text{smooth}}(\mathbf{z}) + G_{\text{front}}(\mathbf{z}) + G_{\text{edge}}(\mathbf{z}) + G_{\text{shock}}(\mathbf{z}) \quad \text{for } \mathbf{z} \in [0,1]^d,$$

where

$$G_{\text{smooth}}(\mathbf{z}) = \sin\left(2\pi\|\mathbf{z}\|\right)$$

$$G_{\text{shock}}(\mathbf{z}) = \left\|S(\mathbf{z}) - \mathbf{z}\right\|$$

$$G_{\text{edge}}(\mathbf{z}) = \begin{cases} S_1(\mathbf{z}), & S(\mathbf{z}) < 0 \\ S_2(\mathbf{z}), & \text{otherwise} \end{cases}$$

$$G_{\text{front}}(\mathbf{z}) = \frac{1}{1 + e^{-S(\mathbf{z})}}.$$

Shallow-Water equations on the sphere

We test using random surface conditions for the shallow-water equations on the rotating sphere in flux form given as

$$\frac{\partial \mathbf{U}}{\partial t} + \frac{\partial \mathbf{F_1}(\mathbf{U})}{\partial x^1} + \frac{\partial \mathbf{F_2}(\mathbf{U})}{\partial x^2} = \mathbf{S}(\mathbf{U}), \tag{5}$$

where the state vector U, the flux vectors F_1 and F_2, and the source term S are defined by

$$\mathbf{U} = \begin{pmatrix} u_1 \\ u_2 \\ \sqrt{G}h \end{pmatrix}, \ \mathbf{F_1}(\mathbf{U}) = \begin{pmatrix} E \\ 0 \\ \sqrt{G}hu^1 \end{pmatrix},$$

$$\mathbf{F_2}(\mathbf{U}) = \begin{pmatrix} 0 \\ E \\ \sqrt{G}hu^2 \end{pmatrix}, \ \mathbf{S}(\mathbf{U}) = \begin{pmatrix} \sqrt{G}u^2(f+\zeta) \\ -\sqrt{G}u^1(f+\zeta) \\ 0 \end{pmatrix}. \tag{6}$$

Shallow-Water equations on the sphere (continued)

Here, $E = \Phi + \frac{1}{2}\left(u_1 u^2 + u_2 u^2\right)$ is defined in terms of the covariant (u_1, u_2) and contravariant (u^1, u^2) wind vectors, with free surface geopotential height (above sea level) given as $\Phi = g(h_s + h)$, where g is the gravitational acceleration, h is the depth of the fluid, and h_s is the height of the underlying topography. The Coriolis force f, divergence δ, and relative vorticity ζ are defined as

$$\delta = \frac{1}{\sqrt{G}}\left[\frac{\partial \sqrt{G} u^1}{\partial x^1} + \frac{\partial \sqrt{G} u^2}{\partial x^2}\right] \quad \text{and} \quad \zeta = \frac{1}{\sqrt{G}}\left[\frac{\partial u_2}{\partial x^1} - \frac{\partial u_1}{\partial x^2}\right]. \quad (7)$$

Electron magnetohydrodynamics: hysteresis bifurcation

We test using the known analytic solution of the two-dimensional, nonlinear, reduced-electron magneto-hydrodynamics model given as

$$\partial_t B_x^* - \nabla \cdot (\mathbf{j}_p B_x^* - \mathbf{B}_p^* j_x) = -\mathcal{D}(\partial_{yx}^2 B_y - \partial_y^2 B_x),$$
$$\partial_t B_y^* - \nabla \cdot (\mathbf{j}_p B_y^* - \mathbf{B}_p^* j_y) = -\mathcal{D}(\partial_{yx}^2 B_x - \partial_x^2 B_y),$$
$$\partial_t B_z^* + d_e^2 (\mathbf{j}_p \cdot \nabla)\nabla^2 B_z + \mathbf{B}_p \cdot \nabla j_z = \mathcal{D}\nabla^2 B_z, \qquad (8)$$

where $\mathbf{B}$ is the magnetic field and $\mathbf{B}^* = \mathbf{B} + d_e^2 \nabla \times (\nabla \times \mathbf{B})$, $\mathcal{D} = \eta - \eta_H \nabla^2$. The quantities η and η_H are the dimensionless resistivity and electron viscosity, respectively, and $d_e = \sqrt{\frac{m_e}{m_i}}$ is the electron inertial length

Contact

Rick Archibald

Computer Science and Mathematics Division
Oak Ridge National Laboratory
(865) 576-5761
archibaldrk@ornl.gov